The 2010 IEEE/RSJ International Conference on
Intelligent Robots and Systems
October 18-22, 2010, Taipei, Taiwan

Determining the Robot-to-Robot 3D Relative Pose using Combinations of Range and Bearing Measurements: 14 Minimal Problems and Closed-form Solutions to Three of them

Xun S. Zhou and Stergios I. Roumeliotis

Abstract— **In this paper, we address the problem of motion-induced 3D extrinsic calibration based on different combinations of inter-robot measurements (i.e., distance and/or bearing observations from either or both of the two robots, recorded across multiple time steps) and ego-motion estimates. In particular, we focus on solving minimal problems where the unknown 6-degree-of-freedom transformation between the two robots is determined based on the minimum number of measurements necessary for finding a discrete set of, in general, multiple solutions. In order to address the very large number of possible combinations of inter-robot observations, we identify symmetries in these problems and use them to prove that any of the possible extrinsic robot-to-robot calibration problems can be solved based on the solution of only 14 (base) minimal problems. Finally, we derive analytical solutions to three of these base problems, and evaluate their performance through extensive simulations.**

I. Introduction

Multi-robot systems (or mobile sensor networks) have attracted considerable attention due to their wide range of applications, such as search and rescue [17], target tracking [11], localization [14], and mapping [9]. In order to accomplish these tasks cooperatively, it is necessary for the robots to share their sensor information. Their measurements, however, are registered with respect to each robot's local reference frame and need to be converted to a common reference frame before they can be fused. This requires knowledge of the robot-to-robot transformation, i.e., their relative position and orientation (pose). Most multi-robot estimation algorithms available today assume that this robot-to-robot transformation is known. However, only few works describe how this transformation can be determined.

One approach to estimating the relative transformation is by *manually* measuring the relative position and orientation between robots. This approach though has several drawbacks. Besides being tedious and time consuming, it might not provide sufficient accuracy and it is inefficient for large robot teams. An alternative method is to use *external references* (e.g., GPS, compass, or a prior map of the environment). However these external references are not always available due to environmental constraints (e.g., underwater, underground, outer space, or indoors).

In the absence of external references, the relative robot-to-robot transformation can be computed using *inter-robot observations*, i.e., robot-to-robot distance and/or bearing measurements. For example, for the case of a *static* sensor network, numerous methods have been proposed for determining the locations of the sensors using distance-only measurements between neighboring sensors [3], [15]. However, these approaches are limited to estimating only the 2D *positions* of static sensors.

In order to estimate the 6-degree-of-freedom (DOF) transformation, the robots will have to move and collect multiple inter-robot measurements. Then the relative pose can be determined using: (i) inter-robot measurements and (ii) the robots' motion estimates. This task of *motion-induced extrinsic calibration* is precisely the problem addressed in this paper. When compared to alternative approaches that rely on external references, motion-induced calibration is more cost efficient since no additional hardware is required, and can be applied in unknown environments where no external aids are available. Additionally, recalibration can be easily carried out in the field when necessary.

In this paper, we focus on solving minimal systems where the number of equations provided by the inter-robot measurements equals the number of unknown parameters. In particular, we consider the case where the robots are equipped with different types of sensors, or record different types of relative measurements over time due to environment constraints. Such minimal problems are formulated as systems of polynomial equations which in general, have multiple (complex) solutions. Even though we are only interested in the unique solution that corresponds to the true relative pose, the minimal solver is extremely useful in practice, especially in the presence of outliers. Specifically, using the minimal number of measurements minimizes the probability of picking an outlier when generating hypotheses within an outlier-rejection scheme such as Random Sample Consensus (RANSAC) [5]. Moreover, the minimal solver can also be used to initialize an iterative process (e.g., nonlinear weighted least squares) for improving the estimation accuracy when additional measurements become available. In particular, a reliable initial estimate can be found by (i) solving several minimal problems, (ii) performing clustering to identify the most probable set of inliers, and (iii) computing the least-squares solution using the inliners.

The main contributions of this paper are twofold:

- We identify 14 base minimal systems. All other problems with different combinations of inter-robot measurements can be solved using the solutions of the base systems.

This work was supported by the University of Minnesota (DTC), and the National Science Foundation (IIS-0643680, IIS-0811946, IIS-0835637).

Xun S. Zhou and Stergios I. Roumeliotis are with the Department of Computer Science and Engineering, University of Minnesota, Minneapolis, MN, 55455 USA email: {zhou|stergios}@cs.umn.edu

- We determine the number of solutions of three minimal systems with mutual bearing measurements, and provide analytic solutions.

The remainder of the paper is organized as follows: After reviewing related work in Section II, we present the problem formulation and the 14 base minimal systems in Section III, and provide solutions for three of these systems in Sections IV and V. The accuracy of the presented methods is evaluated through extensive Monte-Carlo simulations in Section VI, followed by concluding remarks and future work in Section VII.

II. Related Work

Previous work on *extrinsic calibration* of sensor networks using sensor-to-sensor range measurements, has primarily focused on *static* sensors in 2D with the limitation that only their *positions* are determined. Provided that a few anchor nodes can globally localize (e.g., via GPS), the global positions of the remaining nodes can be uniquely inferred if certain graph-rigidity constraints are satisfied [1], [4]. A variety of algorithms based on convex optimization [3], sum of squares (SOS) relaxation [12], and multi-dimensional scaling (MDS) [15] have been employed to localize the sensor nodes in 2D. In 3D, flying anchor nodes have been proposed to localize sensors, e.g., an aerial vehicle aiding static sensor network localization [13], or a single satellite localizing a stationary planetary rover [6]. However, all these schemes only determine the *positions* of *static* sensors.

For many applications (e.g., localization, mapping, and tracking), the knowledge of both relative sensor position *and* orientation is required. Using a combination of distance and bearing measurements to uniquely estimate relative poses in *static* 2D sensor networks was recently shown to be NP-hard [2]. For mobile sensors, the problem of relative pose determination has only been studied thoroughly in 2D. The ability to move and collect measurements from different vantage points provides additional information for localizing the sensors. This information has been shown to make the robots' relative pose observable, given inter-robot distance and/or bearing measurements [10]. Specifically, it is known that mutual distance *and* bearing measurements between two robots from a single vantage point are sufficient to determine the 3-DOF robot-to-robot transformation in closed-form [22], [7]. However, when only distance or bearing measurements are available, the robots must move and record additional observations. Then the relative robot pose can be found by combining the estimated robot motion (e.g., from odometry) and the mutual bearing [10] or distance [23] measurements.

In contrast to the case of motion in 2D, very little is known about motion-induced extrinsic calibration in 3D. Few researchers have addressed the challenging problem of determining relative pose using range-only measurements. Interestingly, in the minimal problem setting, the task of relative-pose estimation using only distance measurements is actually equivalent to the forward-kinematics problem of the general Stewart-Gough platform [16]. This problem has 40 (generally complex) solutions [21], which can be found by solving a system of multivariate polynomial equations [8],

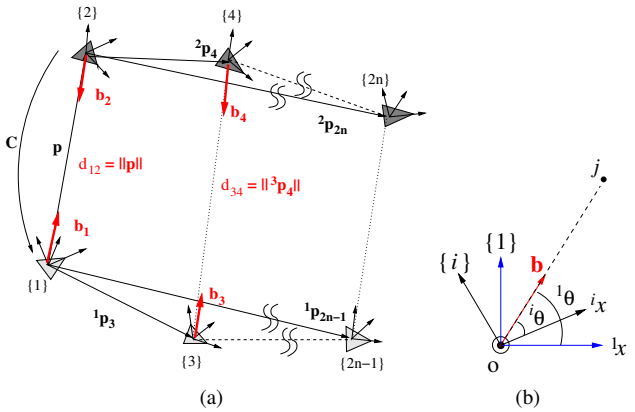

Fig. 1. (a) Geometry of the robot trajectories. The odd (even) numbered frames of reference depict the consecutive poses of robot R_1 (R_2). The distance between the robot poses $\{i\}$ and $\{j\}$ is denoted by d_{ij}, $i \in \{1, 3, \ldots, 2n-1\}$, $j \in \{2, 4, \ldots, 2n\}$. $\mathbf{b}_i$ ($\mathbf{b}_j$) is a unit vector pointing from $\{i\}$ to $\{j\}$ ($\{j\}$ to $\{i\}$) expressed in the initial frame $\{1\}$ ($\{2\}$). The problem is to determine the transformation between the robots' initial frames $\{1\}$ and $\{2\}$, parameterized by the translation vector $\mathbf{p}$ and the rotation matrix $\mathbf{C}$. (b) Illustration of a bearing measurement expressed in different frames of reference. The bearing $\mathbf{b}$ is a unit vector pointing from o to j. When expressed in frame $\{i\}$, the angle between $\mathbf{b}$ and the x-axis of frame $\{i\}$, ^ix, is $^i\theta$. When expressed in frame $\{1\}$, the angle between $\mathbf{b}$ and the x-axis of frame $\{1\}$, ^1x, is $^1\theta$. Transforming the bearing from $\{i\}$ to $\{1\}$ is done by multiplying with the rotation matrix $^1_i\mathbf{C}$: $\mathbf{b}_i = {}^1_i\mathbf{C}\,{}^i\mathbf{b}_j$.

[19]. Moreover, in our recent work [20] we presented methods for estimating the robots' relative pose when both robots measure relative distance and bearing, or bearing only. However, to the best of our knowledge, no algorithms exist for determining 3D relative pose using different *combinations* of robot-to-robot distance and bearing measurements over time, e.g., the robots can measure distance at the first time step, bearing at the second time step, etc. This paper intends to fill this gap. We start our discussion in the next section with the problem formulation and the introduction of the 14 possible minimal systems.

III. Problem Formulation

In order to improve the clarity of presentation, we hereafter describe the notation used in this paper.

$^i\mathbf{p}_j$	Position of frame $\{j\}$ expressed in frame $\{i\}$.
$^i_j\mathbf{C}$	Rotation matrix that projects vectors expressed in frame $\{j\}$ to frame $\{i\}$.
d_{ij}	Distance between the origin of frame $\{i\}$ and $\{j\}$.
$\mathbf{b}_i$	The bearing from robot R_1 to R_2 when R_1 is at pose $\{i\}$, expressed in frame $\{1\}$.
$\mathbf{b}_j$	The bearing from robot R_2 to R_1 when R_2 is at pose $\{j\}$, expressed in frame $\{2\}$.
$s\alpha$	Short for $\sin(\alpha)$.
$c\alpha$	Short for $\cos(\alpha)$.

Consider two robots R_1 and R_2 moving randomly in 3D space through a sequence of poses $\{1\}, \{3\}, \ldots, \{2n-1\}$ for R_1, and $\{2\}, \{4\}, \ldots, \{2n\}$ for R_2 (see Fig. 1). Along their trajectories, the robots can estimate their positions $^1\mathbf{p}_i$ and $^2\mathbf{p}_j$, $i \in \{1, 3, ..., 2n-1\}$, $j \in \{2, 4, ..., 2n\}$, with respect to their initial frames, as well as their orientations, expressed using the rotation matrices $^1_i\mathbf{C}$ and $^2_j\mathbf{C}$ (e.g., by

TABLE I

14 MINIMAL PROBLEMS.

	t_1	t_2	t_3	t_4	t_5	t_6
1	$d_{12}, \mathbf{b}_1, \mathbf{b}_2$	d_{34}				
2	$\mathbf{b}_1, \mathbf{b}_2$	$\mathbf{b}_3$				
3	$d_{12}, \mathbf{b}_1$	$d_{34}, \mathbf{b}_3$				
4	$d_{12}, \mathbf{b}_1$	$d_{34}, \mathbf{b}_4$				
5	$\mathbf{b}_1, \mathbf{b}_2$	d_{34}	d_{56}			
6	$d_{12}, \mathbf{b}_1$	$\mathbf{b}_3$	d_{56}			
7	$d_{12}, \mathbf{b}_1$	$\mathbf{b}_4$	d_{56}			
8	$\mathbf{b}_1$	$\mathbf{b}_3$	$\mathbf{b}_5$			
9	$\mathbf{b}_1$	$\mathbf{b}_3$	$\mathbf{b}_6$			
10	$d_{12}, \mathbf{b}_1$	d_{34}	d_{56}	d_{78}		
11	$\mathbf{b}_1$	$\mathbf{b}_3$	d_{56}	d_{78}		
12	$\mathbf{b}_1$	$\mathbf{b}_4$	d_{56}	d_{78}		
13	$\mathbf{b}_1$	d_{34}	d_{56}	d_{78}	$d_{9,10}$	
14	d_{12}	d_{34}	d_{56}	d_{78}	$d_{9,10}$	$d_{11,12}$

integrating linear and rotational velocity measurements over time). Additionally, at time-step t when robots R_1 and R_2 reach poses $\{i = 2t-1\}$ and $\{j = 2t\}$, respectively, each robot can potentially measure the range and/or bearing towards the other robot. The range between the robots is given by $d_{ij} = ||{}^i\mathbf{p}_j||_2$, and the bearing is described by a unit vector in the current local frame ${}^i\mathbf{b}_j$ for robot R_1 and ${}^j\mathbf{b}_i$ for robot R_2. Later we will also need these unit vectors expressed in their initial frames for which we define $\mathbf{b}_i := {}^1_i\mathbf{C}{}^i\mathbf{b}_j$ and $\mathbf{b}_j := {}^2_j\mathbf{C}{}^j\mathbf{b}_i$. At each time step, the two robots can measure a *subset* of these measurements: $\{d_{ij}, \mathbf{b}_i, \mathbf{b}_j\}$.

Our goal is to use the ego-motion estimates and the relative pose measurements to determine the 6-DOF initial transformation between the two robots, i.e., their relative position $\mathbf{p} := {}^1\mathbf{p}_2$ and orientation $\mathbf{C} := {}^1_2\mathbf{C}$. In this paper, we only focus on solving the minimal problems where the number of measurement constraints equals the number of unknowns. In what follows, we will show that only the 14 systems listed in Table I need to be considered, while all other combinations of inter-robot measurements result into problems equivalent to these 14.

A. All Possible Minimal Problems

We now describe the process to identify these 14 base systems. Note that there are 7 possible combinations of inter-robot measurements at each time step: $\{d_{ij}, \mathbf{b}_i, \mathbf{b}_j\}$, $\{\mathbf{b}_i, \mathbf{b}_j\}$, $\{d_{ij}, \mathbf{b}_i\}$, $\{d_{ij}, \mathbf{b}_j\}$, $\{\mathbf{b}_i\}$, $\{\mathbf{b}_j\}$, $\{d_{ij}\}$, and at most 6 time steps need to be considered if, e.g., only one distance measurement was recorded at each time step. This naive analysis will give us 7^6 cases. Fortunately, we can reduce this number significantly by considering only the minimal problems and using problem equivalence based on the following lemma.

Lemma 1: One instance of the relative pose problem can be transformed to an equivalent problem by the following two operations:

1) Changing the order of the robots.
2) Changing the order of the measurements taken.

Proof: In order to establish problem equivalence, we here demonstrate how to use the solution of the transformed problem (i.e., when the order of the robots or measurements has changed) to solve the original problem (i.e., determine ${}^1_2\mathbf{C}$, ${}^1\mathbf{p}_2$).

First, if we exchange the order of the robots, i.e., rename robot R_2 as R_1 and vice versa, the solution of the transformed problem is $({}^2_1\mathbf{C}, {}^2\mathbf{p}_1)$. Therefore, the solution of the original system is computed from the inverse transformation: ${}^1_2\mathbf{C} = {}^2_1\mathbf{C}^T$, ${}^1\mathbf{p}_2 = -{}^1_2\mathbf{C}^2\mathbf{p}_1$.

Exchanging the order of inter-robot measurements will only make a difference to the problem formulation when the swapping involves measurements recorded at the first time step, since the unknown variables are the 6-DOF initial robot-to-robot transformation. Without loss of generality, assume that measurements taken at the first and second time steps are swapped. Then the solution of the transformed system is actually the transformation $({}^3_4\mathbf{C}, {}^3\mathbf{p}_4)$ between the frames of reference $\{3\}$ and $\{4\}$ of the original system. The solution of the original system can then be computed using: ${}^1_2\mathbf{C} = {}^1_3\mathbf{C}{}^3_4\mathbf{C}{}^2_4\mathbf{C}^T$, and ${}^1\mathbf{p}_2 = {}^1\mathbf{p}_3 + {}^1_3\mathbf{C}{}^3\mathbf{p}_4 - {}^1_2\mathbf{C}{}^2\mathbf{p}_4$. ■

Now we will describe why we only need to consider 14 minimal systems. First of all, we are looking for combinations of measurements that provide 6 equations to determine the 6-DOF transformation, since we are only interested in minimal systems where the number of equations equals the number of unknowns. A distance measurement provides one equation, and a bearing measurement provides two. So we will collect measurements until we accumulate 6 constraints. To keep track of these combinations, we use an expansion tree (see Fig. 2) and prune its branches using Lemma 1.

At the first time step, we can exclude $\{\mathbf{b}_2\}$ and $\{d_{12}, \mathbf{b}_2\}$ from the 7 combinations by changing the order of the robots. Hence, we only need to expand 5 sets of measurements: $\{d_{12}, \mathbf{b}_1, \mathbf{b}_2\}$, $\{\mathbf{b}_1, \mathbf{b}_2\}$, $\{d_{12}, \mathbf{b}_1\}$, $\{\mathbf{b}_1\}$, $\{d_{12}\}$. We will discuss each one of them in the following:

(a) Starting from $\{d_{12}, \mathbf{b}_1, \mathbf{b}_2\}$ we only need to include $\{d_{34}\}$, since all other choices are overdetermined systems [see Fig. 2(a)].
(b) From $\{\mathbf{b}_1, \mathbf{b}_2\}$ we need to consider two cases: $\{\mathbf{b}_3\}$, and $\{d_{34}\}$. Besides removing overdetermined systems, we can also remove $\{\mathbf{b}_4\}$ by exchanging the order of the robots [see Fig. 2(b)]. Moreover, we only need to keep $\{d_{56}\}$ from the possible expansions of $\{d_{34}\}$, since all other problems are overdetermined.
(c) From $\{d_{12}, \mathbf{b}_1\}$ we can exclude two second level expansions from $\{d_{34}\}$ [see Fig. 2(c)], since $\{d_{12}, \mathbf{b}_1; d_{34}; \mathbf{b}_5\}$ and $\{d_{12}, \mathbf{b}_1; d_{34}; \mathbf{b}_6\}$ are equivalent to $\{d_{12}, \mathbf{b}_1; \mathbf{b}_3; d_{56}\}$ and $\{d_{12}, \mathbf{b}_1; \mathbf{b}_4; d_{56}\}$, respectively, by changing the order of the measurements.
(d) Similarly, from $\{\mathbf{b}_1\}$ we can exclude two second level expansions from $\{\mathbf{b}_4\}$, since $\{\mathbf{b}_1; \mathbf{b}_4; \mathbf{b}_5\}$ is equivalent to $\{\mathbf{b}_1; \mathbf{b}_3; \mathbf{b}_6\}$ by changing the order of measurements, and $\{\mathbf{b}_1; \mathbf{b}_4; \mathbf{b}_6\}$ is also equivalent to $\{\mathbf{b}_1; \mathbf{b}_3; \mathbf{b}_6\}$ by first exchanging the order of the robots and then changing the order of measurements. The other cases $\{d_{34}, \mathbf{b}_3, \mathbf{b}_4\}$, $\{\mathbf{b}_3, \mathbf{b}_4\}$, and $\{d_{34}, \mathbf{b}_3\}$ have already been considered in the first three expansions (a)–(c) as root nodes. $\{d_{34}, \mathbf{b}_4\}$ is also considered in (c) after changing the order of the robots.

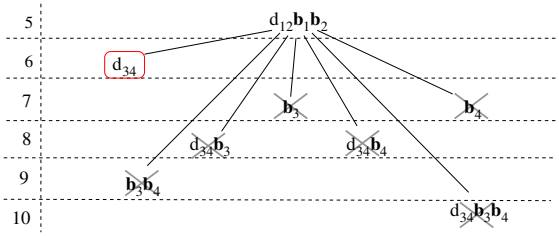

(a) Expansions providing more than 6 constraints are removed.

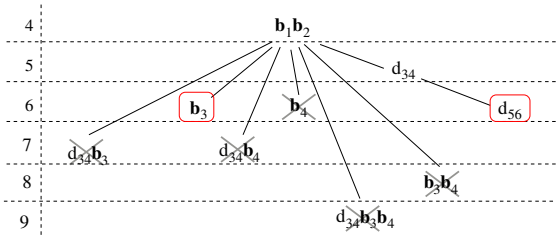

(b) Expansion $\mathbf{b}_4$ is removed since it is equivalent to $\mathbf{b}_3$ by exchanging the order of robots.

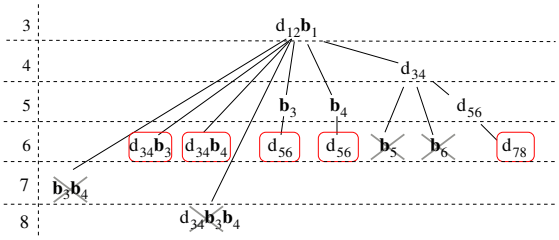

(c) The two combinations $\{d_{12}, \mathbf{b}_1; d_{34}; \mathbf{b}_5\}$ and $\{d_{12}, \mathbf{b}_1; d_{34}; \mathbf{b}_6\}$ are removed since they are equivalent to $\{d_{12}, \mathbf{b}_1; \mathbf{b}_3; d_{56}\}$ and $\{d_{12}, \mathbf{b}_1; \mathbf{b}_4; d_{56}\}$ by changing the order of measurements.

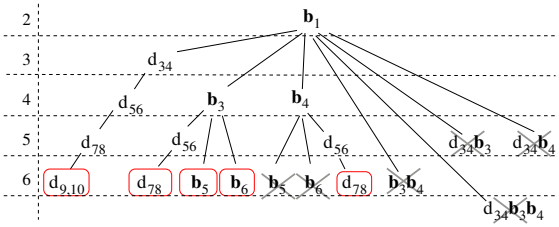

(d) $\{\mathbf{b}_1; \mathbf{b}_4; \mathbf{b}_5\}$ and $\{\mathbf{b}_1; \mathbf{b}_4; \mathbf{b}_6\}$ are equivalent to $\{\mathbf{b}_1; \mathbf{b}_3; \mathbf{b}_6\}$ by changing the order of measurements, or by changing the order of robots and order of measurements. Other nodes: $\{d_{34}, \mathbf{b}_3, \mathbf{b}_4\}$, $\{\mathbf{b}_3, \mathbf{b}_4\}$, $\{d_{34}, \mathbf{b}_3\}$ and $\{d_{34}, \mathbf{b}_4\}$, are removed since they are considered in (a), (b), and (c) as root nodes.

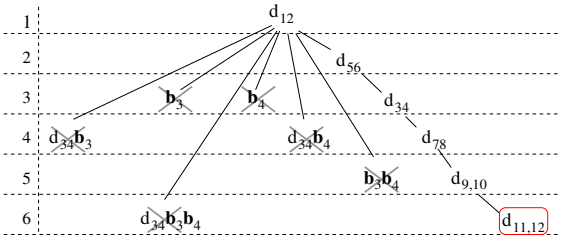

(e) The only case we need is the distance-only case. All other cases have been considered in previous expansions.

Fig. 2. Measurement expansion trees. The numbers on the left of each graph denote the number of constraints provided by the measurements. Since we are only interested in minimal systems, all nodes having more than 6 constraints are removed. The leaf nodes marked by "X" are the ones removed. The nodes marked with red boxes are the 14 base systems. Note that inside { }, the measurements recorded at the same (consecutive) time step are separated by a comma (semicolon).

(e) Finally, for branches expanding from $\{d_{12}\}$, we only need to consider the distance-only case [see Fig. 2(e)], since all other cases have also been considered before.

Adding all the cases together, we have a total of 14 minimal systems listed in Table I.

Next, we will present algebraic solutions to Systems 1, 2, and 5 whose equations share some similarities. Due to limited space, we omit the solutions for Systems 3, 4, and 6–10 and refer to [24] for details. For the remaining systems, we should note that we have addressed System 14 in our previous work [19], while we are currently investigating algebraic and hybrid (numerical/algebraic) methods for solving Systems 11–13.

IV. Algebraic Solutions to the Minimal Problems of Systems 1 and 2

For System 1, we measure $\{d_{12}, \mathbf{b}_1, \mathbf{b}_2; d_{34}\}$, and for System 2, we measure $\{\mathbf{b}_1, \mathbf{b}_2; \mathbf{b}_3\}$. Since the mutual bearing measurements $\mathbf{b}_1$ and $\mathbf{b}_2$ appear in both systems, their equations have similar structure and can be solved using the same approach. In this section, we will first derive the systems of equations for both problems, and then provide their solutions.

A. System 1: Measurements $\{d_{12}, \mathbf{b}_1, \mathbf{b}_2; d_{34}\}$

For this problem, the relative position is directly measured as $\mathbf{p} = d_{12}\mathbf{b}_1$. Therefore, we only need to compute the relative orientation, parameterized by $\mathbf{C}$.

From the mutual bearing measurements $\mathbf{b}_1$ and $\mathbf{b}_2$, we have the following constraint:

$$\mathbf{b}_1 + \mathbf{C}\mathbf{b}_2 = \mathbf{0} \tag{1}$$

Additionally, by expanding the constraint from the distance measurement d_{34}, we have

$$\begin{aligned} {}^3\mathbf{p}_4^{T\,3}\mathbf{p}_4 = (\mathbf{p} + \mathbf{C}\,{}^2\mathbf{p}_4 - {}^1\mathbf{p}_3)^T(\mathbf{p} + \mathbf{C}\,{}^2\mathbf{p}_4 - {}^1\mathbf{p}_3) = d_{34}^2 \\ \Rightarrow \mathbf{v}^T\mathbf{C}\,{}^2\mathbf{p}_4 + a = 0 \end{aligned} \tag{2}$$

where $\mathbf{v} = 2(\mathbf{p} - {}^1\mathbf{p}_3)$ and $a = \mathbf{p}^T\mathbf{p} + {}^2\mathbf{p}_4^{T\,2}\mathbf{p}_4 + {}^1\mathbf{p}_3^{T\,1}\mathbf{p}_3 - 2\mathbf{p}^{T\,1}\mathbf{p}_3 - d_{34}^2$ are known quantities.

The problem now is to find $\mathbf{C}$ from equations (1) and (2). This is described in Section IV-C.

B. System 2: Measurements $\{\mathbf{b}_1, \mathbf{b}_2; \mathbf{b}_3\}$

For this system, besides the mutual bearing constraint (1), we have the following equation using $\mathbf{b}_1$ and $\mathbf{b}_3$, which is the sum of vectors from $\{1\}$, $\{2\}$, $\{4\}$, $\{3\}$ and back to $\{1\}$ (see Fig. 1):

$$\begin{aligned} \mathbf{p} + \mathbf{C}\,{}^2\mathbf{p}_4 - {}^1_3\mathbf{C}\,{}^3\mathbf{p}_4 - {}^1\mathbf{p}_3 = \mathbf{0} \\ \Rightarrow d_{12}\mathbf{b}_1 + \mathbf{C}\,{}^2\mathbf{p}_4 - d_{34}\mathbf{b}_3 - {}^1\mathbf{p}_3 = \mathbf{0}. \end{aligned} \tag{3}$$

If the rotation $\mathbf{C}$ is known, the relative position can be found by first determining the distance d_{12}. To do this, we eliminate d_{34} from equation (3) by forming the cross product with $\mathbf{b}_3$, i.e.,

$$d_{12}\lfloor \mathbf{b}_3 \times \rfloor \mathbf{b}_1 + \lfloor \mathbf{b}_3 \times \rfloor \mathbf{C}\,{}^2\mathbf{p}_4 - \lfloor \mathbf{b}_3 \times \rfloor {}^1\mathbf{p}_3 = \mathbf{0} \tag{4}$$

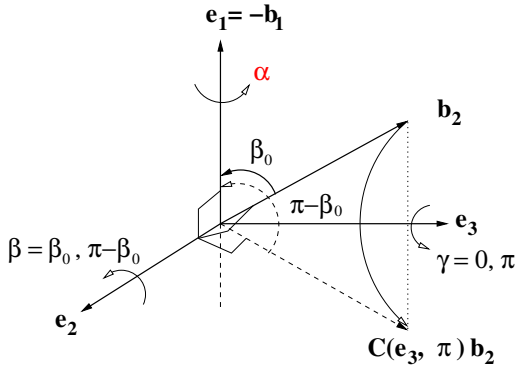

Fig. 3. Two sequences of rotations can satisfy the constraint $\mathbf{b}_1 + \mathbf{C}\mathbf{b}_2 = \mathbf{0}$. Let $\mathbf{e}_1 = -\mathbf{b}_1$, $\mathbf{e}_2 = \frac{\mathbf{b}_2 \times \mathbf{e}_1}{||\mathbf{b}_2 \times \mathbf{e}_1||}$, and $\mathbf{e}_3 = \mathbf{e}_1 \times \mathbf{e}_2$ be three orthonormal rotation axes. Rotating around $\mathbf{e}_2$ by an angle β_0, or first rotating around $\mathbf{e}_3$ by π and then rotating around $\mathbf{e}_2$ by $\pi - \beta_0$, aligns $\mathbf{b}_2$ with $-\mathbf{b}_1$.

where $\lfloor \mathbf{b}_3 \times \rfloor$ is a 3×3 skew-symmetric matrix corresponding to the cross product. Then d_{12} can be computed from (4) by forming the dot product with $\lfloor \mathbf{b}_3 \times \rfloor \mathbf{b}_1$, i.e.,

$$d_{12} = \frac{(\lfloor \mathbf{b}_3 \times \rfloor \mathbf{b}_1)^T \lfloor \mathbf{b}_3 \times \rfloor ({}^1\mathbf{p}_3 - \mathbf{C}^2\mathbf{p}_4)}{(\lfloor \mathbf{b}_3 \times \rfloor \mathbf{b}_1)^T (\lfloor \mathbf{b}_3 \times \rfloor \mathbf{b}_1)} \tag{5}$$

The relative position is then readily available as $\mathbf{p} = d_{12}\mathbf{b}_1$. Next, we will show how to compute $\mathbf{C}$.

The unknown distances d_{12} and d_{34} can be eliminated from equation (3) by projecting it on to the cross product of $\mathbf{b}_1$ and $\mathbf{b}_3$. Let $\mathbf{v} = \mathbf{b}_1 \times \mathbf{b}_3$, forming the dot product with equation (3), then we have:

$$\mathbf{v}^T \mathbf{C}^2 \mathbf{p}_4 - \mathbf{v}^T {}^1\mathbf{p}_3 = 0 \tag{6}$$

If we define a scalar $a := -\mathbf{v}^T {}^1\mathbf{p}_3$, then it is easy to see that equations (6) and (2) have identical structure.

C. Rotation Matrix Determination

We have shown that for both Systems 1 and 2, in order to determine the rotation matrix $\mathbf{C}$, we need to solve the following system of equations:

$$\mathbf{b}_1 + \mathbf{C}\mathbf{b}_2 = \mathbf{0} \tag{7}$$

$$\mathbf{v}^T \mathbf{C}^2 \mathbf{p}_4 + a = 0 \tag{8}$$

The key idea behind our approach is to first exploit the geometric properties of (7) which will allow us to determine two degrees of freedom in rotation. The remaining unknown degree of freedom can subsequently be computed using (8).

Note that in order to satisfy (7), we need to rotate $\mathbf{b}_2$ around a unit vector $\mathbf{e}_2$ perpendicular to both $-\mathbf{b}_1$ and $\mathbf{b}_2$ such that the rotated vector equals to $-\mathbf{b}_1$ (see Fig. 3). Given that a rotation matrix has 3-DOF, we parameterize $\mathbf{C}$ using the rotational angles α, β, and γ around axes $\mathbf{e}_1 = -\mathbf{b}_1$, $\mathbf{e}_2 = \frac{\mathbf{b}_2 \times \mathbf{e}_1}{||\mathbf{b}_2 \times \mathbf{e}_1||}$, and $\mathbf{e}_3 = \mathbf{e}_1 \times \mathbf{e}_2$, respectively. Without loss of generality, assume that $\mathbf{e}_1$, $\mathbf{e}_2$, and $\mathbf{e}_3$ are unit vectors corresponding to the three principal axes,[1] i.e., $\mathbf{e}_1 = [1\ 0\ 0]^T$ etc. Thus, we can write the rotation matrix as:

$$\begin{aligned}\mathbf{C} &= \mathbf{C}(\mathbf{e}_1, \alpha)\mathbf{C}(\mathbf{e}_2, \beta)\mathbf{C}(\mathbf{e}_3, \gamma) \\ &= \begin{bmatrix} 1 & 0 & 0 \\ 0 & c\alpha & -s\alpha \\ 0 & s\alpha & c\alpha \end{bmatrix} \begin{bmatrix} c\beta & 0 & s\beta \\ 0 & 1 & 0 \\ -s\beta & 0 & c\beta \end{bmatrix} \begin{bmatrix} c\gamma & -s\gamma & 0 \\ s\gamma & c\gamma & 0 \\ 0 & 0 & 1 \end{bmatrix}\end{aligned} \tag{9}$$

Next, we will show how to determine the angles γ and β from equation (7).

First, we multiply both sides of (7) with $\mathbf{C}(\mathbf{e}_1, -\alpha)$ to eliminate α:

$$\begin{aligned}&\mathbf{C}(\mathbf{e}_1, -\alpha)\mathbf{b}_1 + \mathbf{C}(\mathbf{e}_1, -\alpha)\mathbf{C}(\mathbf{e}_1, \alpha)\mathbf{C}(\mathbf{e}_2, \beta)\mathbf{C}(\mathbf{e}_3, \gamma)\mathbf{b}_2 = \mathbf{0} \\ &\Rightarrow \mathbf{b}_1 + \mathbf{C}(\mathbf{e}_2, \beta)\mathbf{C}(\mathbf{e}_3, \gamma)\mathbf{b}_2 = \mathbf{0}\end{aligned} \tag{10}$$

Note that $\mathbf{b}_1$ lies along the rotation axis $\mathbf{e}_1$, thus $\mathbf{C}(\mathbf{e}_1, -\alpha)\mathbf{b}_1 = \mathbf{b}_1$.

Then, we form the dot product of both sides of (10) with $\mathbf{e}_2 \perp \mathbf{b}_1$ to eliminate β:

$$\mathbf{e}_2^T \mathbf{C}(\mathbf{e}_3, \gamma)\mathbf{b}_2 = 0 \tag{11}$$

where we have used $\mathbf{e}_2^T \mathbf{b}_1 = 0$ and $\mathbf{e}_2^T \mathbf{C}(\mathbf{e}_2, \beta) = \mathbf{e}_2^T$. Since $\mathbf{e}_2 = [0\ 1\ 0]^T$, and it is perpendicular to $\mathbf{b}_2$, it must be $\mathbf{b}_2 = [b_{2x}\ 0\ b_{2z}]^T$. Substituting these vectors into (11), and employing the structure of $\mathbf{C}(\mathbf{e}_3, \gamma)$ in (9), we have

$$s\gamma b_{2x} = 0 \tag{12}$$

Generally[2] $b_{2x} \neq 0$, therefore $s\gamma = 0$, and thus, $\gamma = 0$ or $\gamma = \pi$. For general configurations, if $\gamma = 0$ then the angle we need to rotate around $\mathbf{e}_2$ to align $\mathbf{b}_2$ with $-\mathbf{b}_1$ is β_0 (see Fig 3). Since these vectors have unit length, $c\beta_0 = \mathbf{b}_2^T \mathbf{e}_1$ and $s\beta_0 = \mathbf{b}_2^T \mathbf{e}_3$. On the other hand, if $\gamma = \pi$, then after rotating $\mathbf{b}_2$ around $\mathbf{e}_3$ by π, the angle between the rotated vector and $\mathbf{e}_1$ is $\pi - \beta_0$.

In summary, for general configurations, we have two solutions for γ and β

$$\gamma = \begin{cases} 0 \\ \pi \end{cases}, \qquad \beta = \begin{cases} \beta_0 & c\beta_0 = \mathbf{b}_2^T \mathbf{e}_1 \\ \pi - \beta_0 & s\beta_0 = \mathbf{b}_2^T \mathbf{e}_3 \end{cases} \tag{13}$$

Next, we will determine the rotation angle α. We first consider the case when $\gamma = 0$ and then follow a similar process to solve for the case when $\gamma = \pi$. It turns out that both cases lead to identical solutions for $\mathbf{C}$.

For $\gamma = 0$ and $\beta = \beta_0$, substituting the expression for $\mathbf{C}$ [see (9)] into (8), we obtain a linear equation in $c\alpha$ and $s\alpha$.

$$\begin{aligned}0 =& \mathbf{v}^T \mathbf{C}(\mathbf{e}_1, \alpha)^2 \mathbf{p}_4' + a \\ =& \underbrace{(v_y p_y' + v_z p_z')}_{l_1} c\alpha + \underbrace{(v_z p_y' - v_y p_z')}_{l_2} s\alpha + \underbrace{v_x p_x' + a}_{l_3} \\ \Rightarrow & c\alpha = -\frac{l_2 s\alpha + l_3}{l_1}\end{aligned} \tag{14}$$

where $\mathbf{v} = [v_x\ v_y\ v_z]^T$, and ${}^2\mathbf{p}_4' = \mathbf{C}(\mathbf{e}_2, \beta_0)^2 \mathbf{p}_4 = [p_x'\ p_y'\ p_z']^T$.

Finally, substituting (14) into the trigonometric constraint $c\alpha^2 + s\alpha^2 = 1$, we get a quadratic polynomial in $s\alpha$.

$$m_0 s\alpha^2 + m_1 s\alpha + m_2 = 0$$

[1] The solution to the general case where $\mathbf{e}_1$, $\mathbf{e}_2$, and $\mathbf{e}_3$ form any other orthonormal basis is described in [24].

[2] If $b_{2x} = 0$, it becomes a singular configuration and we cannot determine the value of γ.

where $m_0 = l_1^2 + l_2^2$, $m_1 = 2l_2l_3$, and $m_2 = l_3^2 - l_1^2$. Back substituting the two solutions for $s\alpha$ into equation (14), we get two solutions for $c\alpha$.

$$s\alpha_1 = \frac{-m_1 + \triangle}{2m_0}, \qquad s\alpha_2 = \frac{-m_1 - \triangle}{2m_0} \tag{15}$$

$$c\alpha_1 = \frac{l_2(m_1 - \triangle)}{2l_1m_0} - \frac{l_3}{l_1}, \; c\alpha_2 = \frac{l_2(m_1 + \triangle)}{2l_1m_0} - \frac{l_3}{l_1} \tag{16}$$

where $\triangle = \sqrt{m_1^2 - 4m_0m_2}$.

For $\gamma = \pi$ and $\beta = \pi - \beta_0$, following the same steps, we again have a linear equation in $c\alpha$ and $s\alpha$:

$$-l_1c\alpha - l_2s\alpha + l_3 = 0 \Rightarrow c\alpha = -\frac{l_2s\alpha - l_3}{l_1} \tag{17}$$

Similarly, substituting the above expression for $c\alpha$ into $c\alpha^2 + s\alpha^2 = 1$, we have

$$m_0s\alpha^2 - m_1s\alpha + m_2 = 0 \tag{18}$$

Hence, we have another two solutions for $s\alpha$ and $c\alpha$ which only have a sign difference compared to the first two solutions.

$$s\alpha_3 = -s\alpha_2, \quad s\alpha_4 = -s\alpha_1 \tag{19}$$

$$c\alpha_3 = -c\alpha_2, \quad c\alpha_4 = -c\alpha_1 \tag{20}$$

Therefore, $\alpha_3 = \alpha_2 - \pi$, and $\alpha_4 = \alpha_1 - \pi$.

Given the relations (19)-(20), the third solution for the rotation matrix $\mathbf{C}$ is:

$$\begin{aligned} &\mathbf{C}(\mathbf{e}_1, \alpha_3)\mathbf{C}(\mathbf{e}_2, \pi - \beta_0)\mathbf{C}(\mathbf{e}_3, \pi) \\ =&\mathbf{C}(\mathbf{e}_1, \alpha_2 - \pi)\mathbf{C}(\mathbf{e}_1, \pi)\mathbf{C}(\mathbf{e}_2, \beta_0) \\ =&\mathbf{C}(\mathbf{e}_1, \alpha_2)\mathbf{C}(\mathbf{e}_2, \beta_0)\mathbf{C}(\mathbf{e}_3, 0) \end{aligned} \tag{21}$$

which is equal to the rotation matrix corresponding to the second solution. One can easily show that the rotation matrix corresponding to the first and fourth solutions are also identical. Therefore, there exist two distinct[3] solutions for the transformation between frames $\{1\}$ and $\{2\}$. In summary, we have the following lemmas for the Systems 1 and 2 (see Table I), respectively.

Lemma 2: Given a pair of mutual bearing measurements ($\mathbf{b}_1$ and $\mathbf{b}_2$) and a distance measurement (d_{12}) recorded at the first location, and an additional distance measurement (d_{34}) between two robots at a different location, there exist two solutions for the 6-DOF robot-to-robot transformation.

Lemma 3: Given a pair of mutual bearing measurements ($\mathbf{b}_1$ and $\mathbf{b}_2$) at the first location, and an additional bearing measurement at a different location ($\mathbf{b}_3$), there exist two solutions for the 6-DOF robot-to-robot transformation.

V. Algebraic Solutions to the Minimal Problem of System 5

In this case,[4] the available measurements are $\{\mathbf{b}_1, \mathbf{b}_2; d_{34}; d_{56}\}$. Using the mutual bearing measurements $\mathbf{b}_1$ and $\mathbf{b}_2$, we can again determine the two rotation angles γ and β [see (13)]. The remaining unknowns α and d_{12} can be computed from the two distance constraints:

$$(d_{12}\mathbf{b}_1 + \mathbf{C}^2\mathbf{p}_4 - {}^1\mathbf{p}_3)^T(d_{12}\mathbf{b}_1 + \mathbf{C}^2\mathbf{p}_4 - {}^1\mathbf{p}_3) = d_{34}^2 \tag{22}$$

$$(d_{12}\mathbf{b}_1 + \mathbf{C}^2\mathbf{p}_6 - {}^1\mathbf{p}_5)^T(d_{12}\mathbf{b}_1 + \mathbf{C}^2\mathbf{p}_6 - {}^1\mathbf{p}_5) = d_{56}^2 \tag{23}$$

After expanding the above two equations, we have a linear system in $c\alpha$ and $s\alpha$. In the case of $\gamma = 0$ and $\beta = \beta_0$, the linear system is

$$l_{11}c\alpha + l_{12}s\alpha + l_{13} = 0 \tag{24}$$

$$l_{21}c\alpha + l_{22}s\alpha + l_{23} = 0 \tag{25}$$

where l_{11}, l_{12}, l_{21}, l_{22} are constant, while l_{13} and l_{23} are quadratic in d_{12}. Note that (24) and (25) do not contain the cross terms $d_{12} \cdot c\alpha$ and $d_{12} \cdot s\alpha$, because $\mathbf{b}_1$ lies on the rotational axis of $\mathbf{C}(\mathbf{e}_1, \alpha)$ and thus $d_{12}\mathbf{b}_1^T\mathbf{C}(\mathbf{e}_1, \alpha) = d_{12}\mathbf{b}_1^T$.

This separation of variables allows us to solve for $c\alpha$ and $s\alpha$ which are again quadratic in d_{12}:

$$\begin{bmatrix} c\alpha \\ s\alpha \end{bmatrix} = \frac{-1}{l_{11}l_{22} - l_{12}l_{21}} \begin{bmatrix} l_{22} & -l_{12} \\ -l_{21} & l_{11} \end{bmatrix} \begin{bmatrix} l_{13} \\ l_{23} \end{bmatrix} \tag{26}$$

Substituting these solutions for $c\alpha$ and $s\alpha$ into $c\alpha^2 + s\alpha^2 = 1$, we arrive at a 4^{th} order univariate polynomial in d_{12}. By back-substitution, each of the four solutions of d_{12} corresponds to one solution for $c\alpha$ and $s\alpha$ [see (26)].

In the case of $\gamma = \pi$ and $\beta = \pi - \beta_0$, following the same procedure as before, yields the same four solutions. Specifically, expanding (22) and (23) we have

$$-l_{11}c\alpha - l_{12}s\alpha + l_{13} = 0 \tag{27}$$

$$-l_{21}c\alpha - l_{22}s\alpha + l_{23} = 0 \tag{28}$$

Hence,

$$\begin{bmatrix} c\alpha \\ s\alpha \end{bmatrix} = \frac{1}{l_{11}l_{22} - l_{12}l_{21}} \begin{bmatrix} l_{22} & -l_{12} \\ -l_{21} & l_{11} \end{bmatrix} \begin{bmatrix} l_{13} \\ l_{23} \end{bmatrix} \tag{29}$$

Compared to (26), they only differ in sign. Invoking the trigonometric constraint $c\alpha^2 + s\alpha^2 = 1$, we arrive at the exact same 4^{th} order univariate polynomial in d_{12}, since the sign does not make a difference after taking squares. Hence, we have the same four solutions for d_{12}. Back-substituting in (29), the solutions for $c\alpha$ and $s\alpha$ will be the negative of the first four solutions. However, the first and second set of four solutions will yield the same rotation matrices [cf. (21)]. In summary, we have the following result for System 5.

Lemma 4: Given a pair of mutual bearing measurements ($\mathbf{b}_1$ and $\mathbf{b}_2$) recorded at the first location, and two distance measurements (d_{34}, d_{56}) recorded at two other locations, the maximum number of solutions for the 6-DOF relative robot-to-robot transformation is four.

VI. Simulation Results

We have evaluated the performance of our algorithms in simulation for different values of inter-robot measurement noise variance. We omit tests on noise in the robots' egomotion estimates, since the effect of perturbing the robots' egomotion estimates is very similar to that of perturbing the inter-robot measurements.

The data for our simulations are generated as follows. First, we generate random robot trajectories, with the two

[3] In case $\triangle = 0$, these two solutions collapse to one.

[4] Due to space limitation, we hereafter provide only an outline of the solution. Detailed derivations are presented in [24].

robots starting at initial positions 1 m $\sim$ 2 m apart from each other, and moving on an average of 3 m $\sim$ 6 m between taking distance and/or bearing measurements. We perturb the true bearing direction to generate the bearing measurements. The perturbed bearing vectors are uniformly distributed in a cone with the true bearing as the axis. The angle between the true vector and the boundary of the cone is defined as σ_b. The noise in the distance measurement[5] is assumed zero-mean white Gaussian with standard deviation $\sigma_d = 10\sigma_b$ m.

We conduct Monte Carlo simulations for different settings of the values of σ_b, and report the averaged results of 10^4 trials per setting for Systems 1, 2, and 5. In all these three systems, we report the error in position as the 2-norm of the difference between the true and the estimated position[6]. To evaluate the error in the relative orientation, we use a multiplicative error model for the quaternion corresponding to the rotation matrix. In particular, true orientation, $\bar{q}$, estimated orientation, $\hat{\bar{q}}$, and error quaternion, $\delta\bar{q}$ are related via [18]:

$$\bar{q} = \delta\bar{q} \otimes \hat{\bar{q}} \tag{30}$$

where $\delta\bar{q}$ describes the small rotation that makes the estimated and the true orientation coincide. Using the small-angle approximation, the error quaternion can be written as

$$\delta\bar{q} \simeq \begin{bmatrix} \frac{1}{2}\delta\boldsymbol{\theta}^T & 1 \end{bmatrix}^T \Leftrightarrow \mathbf{C} \simeq (\mathbf{I}_3 - \lfloor\delta\boldsymbol{\theta}\times\rfloor)\hat{\mathbf{C}} \tag{31}$$

and the 2-norm of $\delta\boldsymbol{\theta}$ is used to evaluate the orientation error.

Fig. 4(a) and Fig. 4(b) show the orientation error and position error as a function of the bearing noise σ_b, respectively. The curves depict the median of the error in the 10^4 trials, and the vertical bars show the 25 and 75 percentiles. As expected, the error increases as the noise increases. We also see an asymmetric distribution of the error around the median for all systems except the position error of System 1. The 75 percentiles are growing much faster than the 25 percentiles. This indicates that the probability of having larger error in the relative pose estimate increases dramatically with the variance of the measurement noise. However, the distribution of the position error of System 1 remains symmetric because it is directly measured from the distance d_{12} and bearing $\mathbf{b}_1$. Finally, we see that in the absence of measurement noise, we can recover the relative pose perfectly.

Fig. 5 shows the frequency (percentage) of the number of real solutions out of the 10^4 trials. We can see that when there is no noise, Systems 1 and 2 always have two real solutions. Because complex solutions appear in pairs for polynomials with real coefficients, if one solution (the one corresponding to the true) is real, then the other must also be real, which is the case when the noise is moderate. However, as the noise variance increases, complex solutions start appearing. This means that perturbing the coefficients may make the real solutions become complex. Also for System 5, when there is no noise, about 25% of the time, there are four real solutions, and 75% of the time, there are two real solutions. But as the noise increases, we start to see cases where no solutions are real. In such cases, we have to discard this set of measurements or take the real part of the complex roots as an approximate solution.

Finally, in all cases the solutions of the minimal problems should be used in conjunction with RANSAC to perform outlier rejection followed by nonlinear least squares so as to improve the estimation accuracy using all available measurements [23].

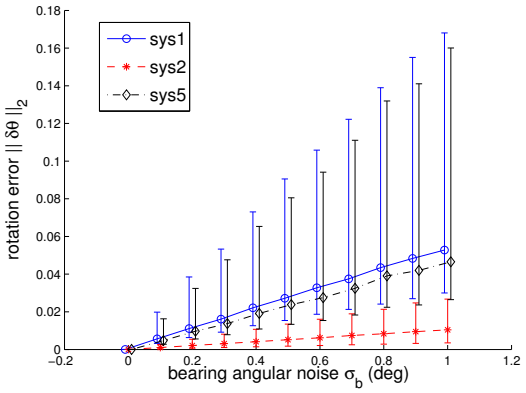

(a) Orientation error

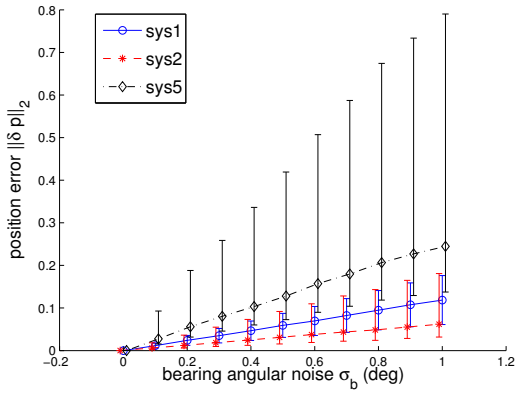

(b) Position error

Fig. 4. Orientation and position errors as functions of the bearing-measurement noise. The plots show the median and 25–75% quartiles in 10^4 random trials.

VII. Conclusion and Future Work

In this paper, we address the problem of computing relative robot-to-robot 3D translation and rotation using inter-robot measurements and known robot motion. We have shown that there exist 14 base minimal systems which result from all possible combinations of inter-robot measurements. Furthermore, we have presented closed-form algebraic solutions to three systems involving mutual robot-to-robot bearing measurements: System 1: $\{d_{12}, \mathbf{b}_1, \mathbf{b}_2; d_{34}\}$, System 2: $\{\mathbf{b}_1, \mathbf{b}_2; \mathbf{b}_3\}$, and System 5: $\{\mathbf{b}_1, \mathbf{b}_2; d_{34}; d_{56}\}$ (see Table I). In particular, we have shown that Systems 1 and 2 have two

[5]Without loss of generality, we assume that only one of the robots records range measurements at each location. If both robots measure the same distance, the two measurements can be combined first to provide a more accurate estimate of their distance.

[6]Since we focus on assessing the accuracy of the minimal problem solver, out of the 2 (or 4) possible solutions, we choose as estimate the one closest to the true value.

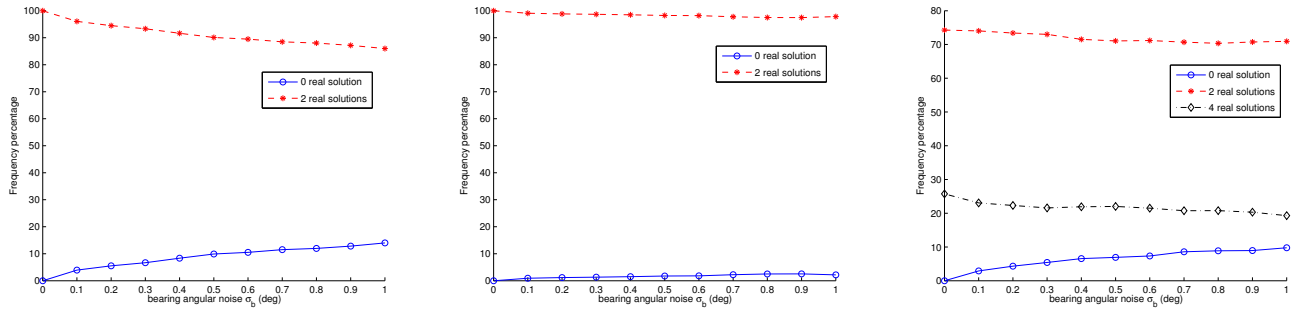

(a) System 1 (b) System 2 (c) System 5

Fig. 5. The frequency (percentage) of cases with 0, 2, or 4 real solutions out of 10^4 trials. Note that for the noise free case, there exist 2 real solutions for Systems 1 and 2, and there exist 2 or 4 real solutions for System 5.

solutions, while System 5 has four solutions for the robot-to-robot transformation. Solutions to some of the remaining problems (Systems 3, 4, 6–10, and 14) are presented in [24] and [19], while solving Systems 11–13 is part of our future work. Finally, we plan to optimize the robot motion such that the uncertainty in the robot-to-robot transformation is minimized. Specifically, our objective is to determine the sequence of locations where the robots will collect the most informative measurements. Following such motion strategies, the time required to achieve the desired level of accuracy will be minimized.

REFERENCES

[1] J. Aspnes, T. Eren, D. K. Goldenberg, A. S. Morse, W. Whiteley, Y. R. Yang, B. D. O. Anderson, and P. N. Belhumeur. A theory of network localization. *IEEE Transactions on Mobile Computing*, 5(12):1663–1678, Dec. 2006.

[2] Y. Dieudonné, O. Labbani-Igbida, and F. Petit. Deterministic robot-network localization is hard. *IEEE Transactions on Robotics*, 26(2):331–339, Apr. 2010.

[3] L. Doherty, K. S. J. Pister, and L. El. Ghaoui. Convex position estimation in wireless sensor networks. In *Proceedings of INFOCOM* 20^{th} *Annual Joint Conference of IEEE Computer and Communications Society*, pages 1655–1663, Anchorage, AK, Apr. 22–26 2001.

[4] T. Eren, D. K. Goldenberg, W. Whiteley, Y. R. Yang, A. S. Morse, B. D. O. Anderson, and P. N. Belhumeur. Rigidity, computation, and randomization in network localization. In *Proceedings of INFOCOM* 23^{rd} *Annual Joint Conference of the IEEE Computer and Communications Societies*, pages 2673–2684, Hong Kong, Mar. 7–11 2004.

[5] M. Fischler and R. Bolles. Random sample consensus: A paradigm for model fitting with application to image analysis and automated cartography. *Communications of the ACM*, 24(6):381–395, June 1981.

[6] S. Higo, T. Yoshimitsu, and I. Nakatani. Localization on small body surface by radio ranging. In *Proceedings of the 16th AAS/AIAA Space Flight Mechanics Conference*, Tampa, FL, Jan. 22–26 2006.

[7] A. Howard, L. E. Parker, and G. S. Sukhatme. Experiments with a large heterogeneous mobile robot team: Exploration, mapping, deployment and detection. *International Journal of Robotics Research*, 25(5–6):431–447, May 2006.

[8] T.-Y. Lee and J.-K. Shim. Improved dialytic elimination algorithm for the forward kinematics of the general Stewart-Gough platform. *Mechanism and Machine Theory*, 38(6):563–577, June 2003.

[9] R. Madhavan, K. Fregene, and L. E. Parker. Distributed heterogeneous outdoor multi-robot localization. In *Proceedings of the IEEE International Conference on Robotics and Automation*, pages 374–381, Washington, DC, May 11–15 2002.

[10] A. Martinelli and R. Siegwart. Observability analysis for mobile robot localization. In *Proceedings of the IEEE/RSJ International Conference on Intelligent Robots and Systems*, pages 1471–1476, Edmonton, Canada, Aug. 2–6 2005.

[11] M. Mazo Jr, A. Speranzon, K. H. Johansson, and X. Hu. Multi-robot tracking of a moving object using directional sensors. In *Proceedings of the IEEE International Conference on Robotics and Automation*, pages 1103–1108, New Orleans, LA, Apr. 26–May 1 2004.

[12] J. Nie. Sum of squares method for sensor network localization. *Computational Optimization and Applications*, 43(2):1573–2894, June 2009.

[13] C.-H. Ou and K.-F. Ssu. Sensor position determination with flying anchors in three-dimensional wireless sensor networks. *IEEE Transactions on Mobile Computing*, 7(9):1084–1097, Sept. 2008.

[14] S. I. Roumeliotis and G. A. Bekey. Distributed multirobot localization. *IEEE Transactions on Robotics and Automation*, 18(5):781–795, Oct. 2002.

[15] Y. Shang, W. Ruml, Y. Zhang, and M. P. J. Fromherz. Localization from mere connectivity. In *Proceedings of MobiHoc* 4^{th} *ACM International Symposium on Mobile Ad Hoc Networking and Computing*, pages 201–212, Annapolis, MD, June 1–3 2003.

[16] D. Stewart. A platform with six degrees of freedom. In *Proceedings of the Institute of Mechanical Engineering*, vol. 180, pages 371–386, 1965.

[17] H. Sugiyama, T. Tsujioka, and M. Murata. Coordination of rescue robots for real-time exploration over disaster areas. In *Proceedings of the* 11^{th} *IEEE International Symposium on Object Oriented Real-Time Distributed Computing (ISORC)*, pages 170–177, Orlando, FL, May 5–7 2008.

[18] N. Trawny and S. I. Roumeliotis. Indirect Kalman filter for 3D attitude estimation. Technical Report 2005-002, University of Minnesota, Dept. of Comp. Sci. & Eng., Jan. 2005.

[19] N. Trawny, X. S. Zhou, and S. I. Roumeliotis. 3D relative pose estimation from six distances. In *Proceedings of Robotics: Science and Systems*, Seattle, WA, June 28 – July 1 2009.

[20] N. Trawny, X. S. Zhou, K. X. Zhou, and S. I. Roumeliotis. Interrobot transformations in 3D. *IEEE Transactions on Robotics*, 26(2):225–243, Apr. 2010.

[21] C. W. Wampler. Forward displacement analysis of general six-in-parallel SPS (Stewart) platform manipulators using soma coordinates. *Mechanism and Machine Theory*, 31(3):331–337, Apr. 1996.

[22] X. S. Zhou and S. I. Roumeliotis. Multi-robot SLAM with unknown initial correspondence: The robot rendezvous case. In *Proceedings of the IEEE/RSJ International Conference on Intelligent Robots and Systems*, pages 1785–1792, Beijing, China, Oct. 9–15 2006.

[23] X. S. Zhou and S. I. Roumeliotis. Robot-to-robot relative pose estimation from range measurements. *IEEE Transactions on Robotics*, 24(6):1379–1393, Dec. 2008.

[24] X. S. Zhou and S. I. Roumeliotis. Determining the robot-to-robot relative pose using range and/or bearing measurements. Technical report, University of Minnesota, Dept. of Comp. Sci. & Eng., MARS Lab, Feb. 2010. [Online]. Available: www.cs.umn.edu/~zhou/paper/14systech.pdf